Quasiparticles in heavy-fermion systems with nearly integer valence

1996 J. Phys.: Condens. Matter 8 3601

(http://iopscience.iop.org/0953-8984/8/20/007)

J. Phys.: Condens. Matter **8** (1996) 3601–3617. Printed in the UK

Quasiparticles in heavy-fermion systems with nearly integer valence

K A Kikoin

Russian Research Center 'Kurchatov Institute', 123182 Moscow, Russia

Received 11 December 1995

Abstract. The theory describing the electron mass enhancement in Kondo-lattice heavy-fermion systems is presented. The description is based on the picture of a spin Fermi liquid of RVB type which strongly interacts with conduction electrons. It is shown that the electron–spinon scattering results in large phase shifts for conduction electrons near the Fermi level which mimic the resonance renormalization but does not involve f-electron states. The results are compared with dHvA data for several Ce-based compounds.

1. Introduction

It is generally accepted that the eventual source of unusually high density of states of fermionic excitations which is observed experimentally in numerous uranium- and cerium-based heavy-fermion (HF) materials is the involvement of internal degrees of freedom of unfilled f shells of these elements in the low-energy excitation spectra. However, the mechanism of strong effective mass enhancement in these materials is still a matter of discussion. Recently it became clear (see, e.g., [1]) that one should discriminate between the intermetallic compounds with non-integer valence where the f-electrons are directly involved in metallic cohesion and charge transport via hybridization with the less tightly bound valence electrons, and those systems which demonstrate nearly integer valence. In the latter case the charge fluctuations in the f channel are suppressed, and only spin degrees of freedom are easily excited at low energy and temperature. Most of the U-based HF systems, such as UBe_{13}, UPt_3, and URu_2Si_2, and some Ce-based materials ($CeSn_3$, $CeNi_5$, CeNi), apparently, belong to the first group. But there are many examples of practically integer-valent compounds such as $CeAl_2$, $CeAl_3$, $CeIn_3$, $CeCu_6$, and maybe $CeRu_2Si_2$ which demonstrate all characteristic features of HF systems in a 'Kondo lattice' regime when the charge excitations involving the electrons from the f shell seem to be forbidden due to strong intraatomic Hubbard repulsion.

It was argued in [2] that the most of the experimental methods available do not allow one to determine the degree of involvement of f-electrons in the thermodynamic and even in the transport properties of HF materials. In this situation the experimental methods which deal exclusively with charge excitations seem to play a part of *experimentum crucis* in the problem of the origin of heavy-fermion behaviour. Among these methods the studies of de Haas–van Alphen oscillations gave until recently the most useful information. In particular, the dHvA studies of extremal cross sections of the Fermi surface and the corresponding effective masses of the carriers in UPt_3 [3] resulted both in fairly good agreement with the data of band calculations of the Fermi surface topology and in registering genuinely large

0953-8984/96/203601+17$19.50

effective masses which could be ascribed to the f electrons at the Fermi level. On the other hand, there are numerous examples of dHvA measurements in HF materials, such as UBe_{13} [4] and $CeCu_2Si_2$ [5], where the large masses were not observed at all. The most interesting is the situation with two non-magnetic, non-superconducting materials $CeCu_6$ and $CeRu_2Si_2$ which belong to the group of nearly-integer-valent HF systems. In both these materials large effective masses were found. The value of $m^* \approx 80m_0$ was observed in $CeCu_6$ [6] and the extremely large mass of $m^* \approx 140m_0$ was seen in $CeRu_2Si_2$ [7, 8]. The latter system is an unique object for studying the electron mass enhancement effect because it allows dHvA measurements in a wide range of magnetic field values and directions, and the information obtained could be compared with theoretical calculations of electron spectra. It was found (see [9] for a review) that the general shape of the Fermi surface is formed by the usual metallic bands, but the huge effective mass found experimentally for two electron sheets of the Fermi surface cannot be described without appealing to strong correlation effects.

The conventional methods of theoretical description of strong correlation effects in band structure calculations originate from the idea of Abrikosov–Suhl resonance as a final source of strong renormalization of the electron effective mass at the Fermi surface [10, 11, 12]. According to this approach, the Kondo scattering results in formation of the resonance at nearly zero energy in *each* site of the Kondo lattice which means that the phase shift $\delta_{l=3}(\epsilon)$ for the scattering of conduction electron on each f atom is close to $\pi/2$ at $\epsilon \to \epsilon_F$. In spite of the definitely spin origin of the Abrikosov–Suhl resonance in the original single-site Kondo problem, the mean-field approximation used in the procedures of transforming this resonance into the extremely narrow band just above the Fermi surface (see [13] for detailed description of the theory) includes an important step of charge transfer from conduction electrons to spin degrees of freedom representing f ions [14, 2].

In the present paper another possibility of obtaining strong mass enhancement and the change of the topology of Fermi surface is described. The mechanism of spin–charge scattering described below is based on the same Kondo lattice Hamiltonian, but the approach proposed does not appeal to the Kondo resonance and does not demand a phenomenological extra narrow f level above the Fermi level. This scattering is potential in its origin and character but, nevertheless, it results in renormalization of both Fermi surface and effective masses of charged carriers. The conclusions of the theory are compared with the experimental data for different HF materials.

2. General theory of electron–spinon scattering

We consider the Kondo lattice Hamiltonian

$$H = H_0 + H_{int} = \sum_{\boldsymbol{k},\nu\sigma} \epsilon^{\nu}_{\boldsymbol{k}} a^{+}_{\boldsymbol{k}\sigma\nu} a_{\boldsymbol{k}\sigma\nu} + 2J \sum_{\boldsymbol{i},\nu} \left(\boldsymbol{S_i} \cdot \boldsymbol{s}^{\nu}_{\boldsymbol{i}} + \frac{1}{4} \sum_{\sigma} a^{+}_{\boldsymbol{i}\sigma\nu} a_{\boldsymbol{i}\sigma\nu} \right). \tag{1}$$

Here H_0 is the Hamiltonian describing the states in conduction bands, ν is the band index, and H_{int} is the Hamiltonian of contact exchange interaction between the conduction electrons and the localized spins $S = 1/2$ in the sites $\boldsymbol{i}$ of the Kondo lattice. Thus the f-electron subsystem is represented in this Hamiltonian only by the localized spins $\boldsymbol{S_i}$ which interact with itinerant moment $\boldsymbol{s}^{\nu}_{\boldsymbol{i}} = \frac{1}{2} \sum_{\boldsymbol{k}\boldsymbol{k}',\nu\sigma\sigma'} a^{+}_{\boldsymbol{k}\sigma\nu} \hat{\tau} a_{\boldsymbol{k}'\sigma'\nu}$ of conduction electrons ($\hat{\tau}$ is the Pauli matrix). H_{int} can be represented in conventional quartic form

$$H_{int} = J \sum_{\boldsymbol{j},\sigma\sigma'} \sum_{\boldsymbol{k}\boldsymbol{k}',\nu} f^{+}_{\boldsymbol{j}\sigma} f_{\boldsymbol{j}\sigma'} a^{+}_{\boldsymbol{k}\sigma'\nu} a_{\boldsymbol{k}'\sigma\nu} \, \mathrm{e}^{\mathrm{i}(\boldsymbol{k}-\boldsymbol{k}')\boldsymbol{R}_j} \tag{2}$$

by returning to Fermi operators $f^{+}_{\boldsymbol{j}\sigma'}$, $f_{\boldsymbol{j}\sigma'}$ which describe the localized f electrons. The sign of exchange constant corresponds to the antiferromagnetic coupling.

Since the charge fluctuations in a Kondo lattice are forbidden for f electrons by strong intra-site Hubbard repulsion, the f operators in the Hamiltonian (2) can be treated as Abrikosov pseudofermions which describe the spin excitations and carry no charge. Then, the indirect intersite RKKY interaction which appears in the Kondo lattice as a result of exchange by virtual electron–hole pairs can be responsible for both the spin ordering transition and spin liquid formation. The Abrikosov–Suhl resonance near the Fermi level was shown to be the source of stabilization of the spin-liquid resonating valence bond (RVB) state [14]. In the mean-field approximation this Kondo-stabilization mechanism is described by the following decoupling of the Hamiltonian (2),

$$H_{int} = J \sum_{j,\nu} \sum_{k,\nu\sigma} [\Delta_j f^+_{j\sigma} a_{k\sigma\nu} \mathrm{e}^{-\mathrm{i}k\cdot R_j} + \mathrm{HC}] \tag{3}$$

where the anomalous correlator

$$\Delta_j = N^{-1} \sum_{k\sigma} \langle f_{j\sigma} a^+_{k\sigma} \rangle \mathrm{e}^{\mathrm{i}k\cdot R_j} = \sum_{\sigma} \langle f_{j\sigma} a^+_{j\sigma} \rangle \tag{4}$$

is introduced. Then, assuming $\Delta_j = \Delta_0$ to be a site-independent real quantity one comes to the effective hybridization Hamiltonian where the f fermions which described initially neutral spin states acquire charge (see, e.g., [14, 2]), and the characteristic 'hybridization intergral' can be estimated as

$$V_0 = J\Delta_0 \approx (\epsilon_F T_K)^{(1/2)} \tag{5}$$

where T_K is the Kondo temperature and ϵ_F is the Fermi energy.

However, it was shown in [15] that another scenario can be realised in a critical region $T_N(\alpha_c) \approx T_K(\alpha_c)$ of the Doniach's phase diagram. This diagram [16] describes the dependence of competing Néel and Kondo temperatures, $T_N \sim \alpha^2$ and $T_K \sim \exp(-\alpha^{-1})$ on the coupling constant $\alpha = 2J\mathcal{N}(\epsilon_F)$ (here $\mathcal{N}(\epsilon_F)$ is the density of states on the Fermi surface). This scenario predicts that at $\alpha \sim \alpha_c$ the spin liquid phase of RVB type can arise at $T \approx T^* > T_N > T_K$ due to the fact that the Kondo scattering processes reduce noticeably the Néel temperature T_N in this region (see, e.g., [1]) whereas the temperature T^* of RVB ordering is not violated by Kondo sceening.

This means that the f spins which behave as the localized moments $S_j = \frac{1}{2} f^+_{j\sigma} \hat{\tau} f_{j\sigma'}$ at high temperature are transformed into uniform RVB excitations

$$b_{ij} = \sum_{\sigma} f^+_{i\sigma} f_{j\sigma} \tag{6}$$

at $T \sim T^*$ so that $r = \ln(T^*/T_K) \gtrsim 1$. At this temperature the one-site exchange is noticeably enhanced at $T \simeq T^*$ by Kondo scattering processes,

$$\tilde{J}(\epsilon, T) \approx \frac{J}{1 - \alpha \ln \epsilon_F / \max(\epsilon, T^*)} \sim \frac{\epsilon_F}{r}. \tag{7}$$

The transformation from the regime of nearly free paramagnetically disordered local spins to a spin-liquid RVB state has a crossover character provided the gauge field fluctuations are properly taken into account (see, e.g., [17]), but in any case the Kondo scattering processes are quenched at $T \sim T^*$ in accordance with (7). This means that the f spins are only partially screened by exchange interaction with conduction electrons and the full-scale Kondo singlet states characterized by the parameter Δ_0 are not formed at low temperatures. The interaction between the 'slow' electrons with the energies $|\epsilon - \epsilon_F| < T^*$ and the spin excitations is still described by exchange interaction Hamiltonian (2)

$$\tilde{H}_{int} = \tilde{J} \sum_{j,\nu} \sum_{\sigma\sigma'} f^*_{j\sigma} f_{j\sigma'} a^+_{j\sigma'\nu} a_{j'\sigma\nu} \tag{8}$$

but with two essential reservations: (i) the renormalized coupling constant $\tilde{J} \equiv \tilde{J}(0, T^*)$ (7) dressed by the fast excitations with $|\epsilon - \epsilon_F| > T^*$ enters $\tilde{H}_{int}$ instead of the bare coupling constant J and (ii) the Fermi operators $f_{j\sigma}$ now describe the spinon excitations in a narrow band with the width of $\simeq T^*$ [14]. These fermions obey the kinematic constraint

$$\sum_{\sigma} f^{+}_{j\sigma} f_{j\sigma} = 1 \tag{9}$$

and thus possess particle–hole symmetry.

Now we turn to calculation of the electron effective mass enhancement due to strong electron–spinon scattering. This scattering gives both static and dynamical contributions to renormalization of the low-energy electron spectrum for the self-energy part of the electron Green function

$$G_{k\nu}(\omega) = (\omega - \epsilon_{k\nu} - \Sigma_{k\nu}(\omega))^{-1} \tag{10}$$

which are given by the diagrams of figures 1 and 2, respectively (spin index is omitted because we consider here only spin-diagonal processes). The first diagram describes the static scattering which is given by the last term of the interaction Hamiltonian (1). This scattering is negligible for fast electrons, but the slow carriers strongly interact with spinons, and the static scattering amplitude which is characterized by the potential $\tilde{J}/2$ should be taken into account in the periodic lattice potential $V_{gg'}$ for conduction electrons ($\boldsymbol{g}$ is the reciprocal lattice vector). The second diagram describes the spinon scattering contribution to electron self-energy $\Sigma_{k\nu}(\omega)$ in the Born approximation. The latter contribution is usually considered in any discussion of heavy-electron mass renormalization due to interaction with Bose fields of different origin existing in a narrow energy interval $\bar{\omega} \ll \epsilon_F$ (see, e.g., [18–23]). We will return to this term after discussing the one-site contribution given by the diagram of figure 1.

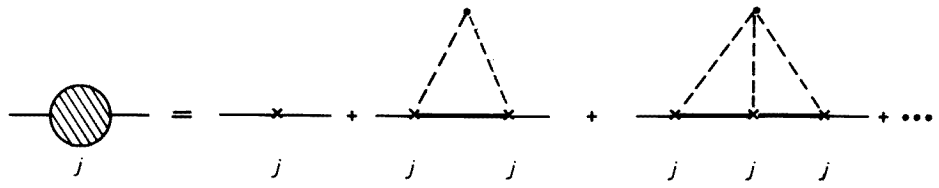

Figure 1. One-site scattering amplitude T_j for conduction electron self-energy.

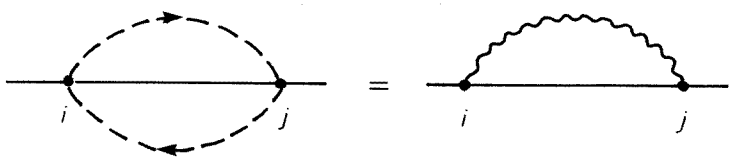

Figure 2. Second-order contribution to conduction electron self-energy. The dashed lines represent the spinon Green functions and the wavy line stands for the polarization operator Π_{ij}.

One could expect that the static contribution will modify strongly the dispersion law for conduction electrons in a narrow interval of energies $\sim T^*$ since the magnitude of the scattering potential which is determined by the coupling constant $\tilde{J} \sim \epsilon_F / \ln(T^*/T_K)$ (see

(7)) is comparable with the energy of incident Bloch waves. Hence, the full scattering amplitude $T_{gg'}$ which is denoted by the hatched circle in figure 1 should be taken into account in the calculations of spinon contribution to the periodic scattering potential. Only the spin-diagonal part of the electron–spinon interaction enters this potential (provided we are far enough from any magnetic instability), so the constraint (9) allows one to ascribe the value of $\tilde{J}/2$ to the bare vertices marked by the crosses in figure 1. The dotted lines which connect the crosses mean that all vertices are related to the same lattice site.

The scattering amplitude for one-site scattering potential is easily calculated (see [24]). In a coordinate representation it has the form

$$T_j = \frac{\tilde{J}_j}{1 - M(\epsilon)} \tag{11}$$

where

$$M(\epsilon) = \frac{\tilde{J}}{2}\int \mathrm{d}E \frac{\mathcal{N}_v(E)}{\epsilon - E + \mathrm{i}\delta} = \frac{J}{2}[R(\epsilon) - \mathrm{i}\pi\mathcal{N}_v(\epsilon)]. \tag{12}$$

Only those 'slow' electrons with $E < T^*$ which are subject to strong Kondo-enhanced scattering give a contribution to this integral. $\mathcal{N}_v(E)$ is the density of states of these electrons; $R(\epsilon)$ is the real part of the integral $M(\epsilon)$. The scattering amplitude

$$T_{gg'}(\boldsymbol{k}) = (\boldsymbol{k} + \boldsymbol{g}|T_j|\boldsymbol{k} + \boldsymbol{g}') \tag{13}$$

should be substituted in a secular equation for the band structure calculation together with the ordinary scattering potential

$$V_{gg'} = \int V_j(\boldsymbol{r}) \exp \mathrm{i}(\boldsymbol{g} - \boldsymbol{g}')(\boldsymbol{r} - \boldsymbol{R}_j). \tag{14}$$

At this stage it is convenient to turn to a spherical muffin-tin (MT) approximation for the lattice potential because this approximation was used in all preceding semi-phenomenological band structure calculations for the Kondo lattices which stem from the work [12]. Then the scattering amplitude is expressed via partial wave phase shifts $\delta_l(\epsilon)$ on the boundary of the MT sphere. The Green function calculations result in this case in a well known secular equation (the so called KKRZ equation, see [25])

$$\left|\left(\frac{|\boldsymbol{k} - \boldsymbol{g}|^2}{2m_0} - \epsilon\right)\delta_{gg'} - \Gamma_{gg'}\right| = 0 \tag{15}$$

where the matrix element of the potential scattering has the form

$$\Gamma_{gg'} = \frac{4\pi}{2m_0\kappa\Omega_0}\sum_l (2l+1)\tan\eta_l \frac{j_l(|\boldsymbol{k} - \boldsymbol{g}|R)\, j_l(|\boldsymbol{k} - \boldsymbol{g}'|R)}{j_l(\kappa R)\, j_l(\kappa' R)} P_l(\cos\theta_{gg'}). \tag{16}$$

Here Ω_0 is the unit volume, R is the radius of the MT sphere, $\kappa = \sqrt{2m_0\epsilon}$, $P_l(x)$ is the Legendre polynomial, $j_l(x)$ and $n_l(x)$ are the spherical Bessel and Neumann functions, respectively. The phase shift δ_l enters equation(16) via

$$\cot\eta_l(\kappa) = \cot\delta_l(\kappa) - n_l(\kappa R)/j_l(\kappa R). \tag{17}$$

The phase shift due to spinon potential scattering can be found from the scattering amplitude $T_j(\epsilon)$ given by (11),

$$\tan\delta_l(\epsilon) = \frac{\pi\tilde{J}\mathcal{N}(\epsilon)}{2 - \tilde{J}R(\epsilon)}. \tag{18}$$

At this point our calculation of spinon contribution to the electron band states could be compared with those of the resonance scattering theory.

The theory of the renormalized band structure of Kondo lattices (see [9] and references therein) adopts for the phase shift in the f channel ($l = 3$) the resonance form

$$\delta_3(\epsilon) = \tan^{-1} \frac{T_K}{\epsilon_0 - \epsilon}. \tag{19}$$

This phenomenological assumption is substantiated by the idea that the one-site scattering amplitude in this channel is enhanced by extra spin-fluctuation scattering of Kondo origin which is known to result in a resonance behaviour of a phase shift in a single-impurity case,

$$\delta_l(\epsilon) = \delta_l(\epsilon_F) + T_K^{-1}(\epsilon - \epsilon_F) \tag{20}$$

where $\delta_l(\epsilon_F) = \pi/N$, and N is the number of scattering channels. It is believed in this approach that the Kondo lattice could be approximated by the lattice of uncorrelated Kondo singlet states, and, as a result, the effective 'resonance level' ϵ_0 appears which position is to be found from the Friedel sum rule (or electrical neutrality condition). As a result, the electron excited from the Fermi sea sees a narrow resonance just above the Fermi surface, $\epsilon_0 - \epsilon_F = bT_K$, $b \sim 1$ in accordance with (19).

Then, substituting (19) into secular equation (15) one comes to a familiar picture of a narrow band hybridized with nearly free conduction bands. If one neglects the angular dependence of resonance scattering, the equation (15) can be rewritten for a single-channel scattering case as

$$\left| \left(\frac{|\boldsymbol{k} - \boldsymbol{g}|^2}{2m_0} - \epsilon \right) \delta_{gg'} - \frac{V_0^2 B_g B_{g'}}{\epsilon_0' - \epsilon} \right| = 0 \tag{21}$$

where

$$\epsilon_0' - \epsilon_F = T_K \left[b - \frac{n_3(\kappa R)}{j_3(\kappa R)} \right] \tag{22}$$

the parameter V_0 is defined in (5), and

$$B_g = \left(\frac{2\pi}{m_0 \kappa \Omega_0 \epsilon_F} \right)^{1/2} \frac{j_3(|\boldsymbol{k} - \boldsymbol{g}|R)}{j_3(\kappa R)}. \tag{23}$$

Since the spin f states have picked a charge up in the process of transformation of exchange Hamiltonian (2) to effective hybridization Hamiltonian (3) the Friedel sum rule

$$\Delta n = \frac{N}{\pi} \delta(\epsilon_F) \sim 1 \tag{24}$$

demands a noticeable drop of the chemical potential $\Delta\mu \sim T_K$. As a result, not only are the effective mass and the Fermi wave vector strongly renormalized due to resonance Kondo scattering (figure 3(a)), but also the electronic compressibility should suddenly increase when T passes T_K because the extra heavy electron appears under the Fermi surface at $T < T_K$. This result is an undesirable consequence of the resonance approach which could hardly be avoided in phenomenological calculations of this type [26], although a more refined many-body treatment overcomes this difficulty [19, 9].

Let us compare these results with the changes which arise in the low-energy electron excitation spectrum due to strong electron–spinon scattering. The phase shift given by (18) should be inserted in KKRZ secular equation (15) instead of (19). However, in this case only those electrons which give the dominant contribution to the local exchange interaction are subject to strong exchange scattering. These are the d electrons donated by Ce ions and neighbouring Ru ions into the conduction band. Hence, one should examine those sheets of the Fermi surface which have a noticeable contribution of the $d_{Ce,Ru}$ partial wave with

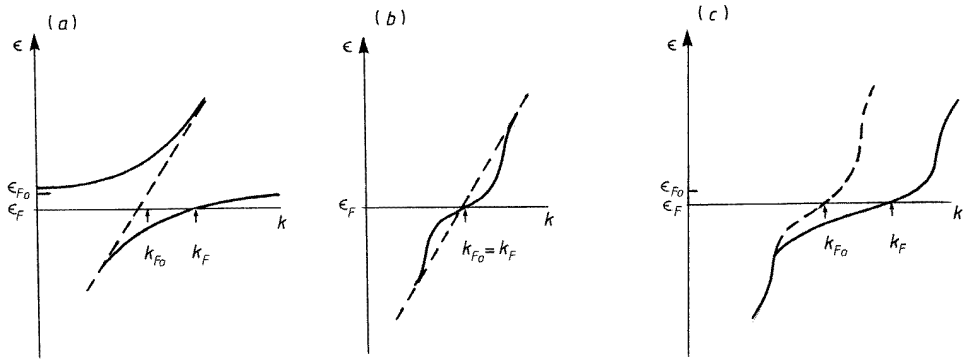

Figure 3. Renormalization of the conduction electron dispersion law near the Fermi surface: (*a*) due to Kondo-resonance interaction; (*b*) due to Migdal-type non-adiabatic interaction; (*c*) due to Migdal-type interaction plus static exchange scattering.

$l = 2$. We simplify the problem for illustrative purposes and consider here the case of a single Bloch wave subject to strong spinon renormalization.

It should be emphasized that the two contributions to electron dispersion renormalization given by the diagrams of figures 1 and 2 should be considered together because both mechanisms influence the electrons in the same thin layer with the width of T^* around the Fermi surface. This is why the full lines which correspond to the electron Green functions given by (10) with the self-energy part depicted in figure 2 should be substituted into the diagram of figure 1. As mentioned above, the calculation of the former diagram is a well known procedure. In the context of HF theory the effective mass renormalization of this type was calculated, e.g., in [19–22]. So we recall here in brief the calculation scheme.

Using the Matsubara Green function technique the self-energy part of figure 2 can be written as

$$\Sigma(\boldsymbol{p}, \varepsilon_n) = \tilde{J}^2 T \sum_m \int \frac{\mathrm{d}\boldsymbol{p}'}{(2\pi)^3} \frac{\Pi(\boldsymbol{p}-\boldsymbol{p}', \omega_m)}{\mathrm{i}\varepsilon_{n-m} - \xi_{\boldsymbol{p}'} - \Sigma(\boldsymbol{p}, \varepsilon_{n-m})} \tag{25}$$

where $\varepsilon_n = (2n+1)\pi T$ and $\omega_m = 2m\pi T$ are Matsubara frequencies, $\boldsymbol{p} = \hbar\boldsymbol{k}$, $\xi_{\boldsymbol{p}} = v_F(\boldsymbol{p}-\boldsymbol{p}_F)$ is the electron quasiparticle energy, $\Pi(\boldsymbol{q}, \omega_m)$ is the polarization operator which is given by the spinon particle–hole pair propagator. This polarization loop can be represented as

$$\Pi(\boldsymbol{q}, \omega_m) = \int_0^\infty \mathrm{d}E\, P(\boldsymbol{q}, E) \frac{2E}{\omega_m^2 + E^2} \tag{26}$$

where $P(\boldsymbol{q}, E)$ is a spectral density which characterizes the spin-fermion liquid. Since we are interested only in small ξ, the $\mathrm{d}\boldsymbol{p}'$ integration can be carried separately over the energy $\xi_{\boldsymbol{p}'}$ and the momentum direction $\boldsymbol{p}'/p'$ on the Fermi surface. Then, in a first approximation in $(r)^{-2} = (\tilde{J}/\epsilon_F)^2$ one comes to the universal expression for the self-energy [21, 22],

$$\Sigma(\boldsymbol{p}, \varepsilon_n) = -\mathrm{i}\pi \mathcal{N}_0(\epsilon_F) \tilde{J}^2 T \sum_{m=-n}^{n} \langle \Pi(\boldsymbol{p}-\boldsymbol{p}', \omega_m) \rangle \tag{27}$$

where $\langle \ldots \rangle$ stands for the average over the angle between $\boldsymbol{p}$ and $\boldsymbol{p}'$ on the Fermi surface, and $\mathcal{N}_0$ is the density of states of bare electrons. Then, turning to the limit $T \to 0$ and

making the analytical continuation, one finds from (27) the simple equation for the real part Σ_R of the self-energy,

$$\Sigma_R(\boldsymbol{p}, \varepsilon) = -\mathcal{N}_0(\epsilon_F)\tilde{J}\varepsilon\langle\Pi_0\rangle. \tag{28}$$

The Green function (10) with the self-energy given by the diagram of figure 2 behaves near the Fermi surface as

$$G(\boldsymbol{p}, \varepsilon) = \frac{Z}{\varepsilon - Z\boldsymbol{v}_F(\boldsymbol{p} - \boldsymbol{p}_F)} \tag{29}$$

where the factor $Z^{-1} = (1 + \lambda)$ characterizes the mass enhancement

$$m^* = m_0(1 + \lambda_\varepsilon) \qquad \lambda_\varepsilon = -\frac{\mathrm{d}\Sigma_R(\varepsilon)}{\mathrm{d}\varepsilon}. \tag{30}$$

Using (28) one comes finally to the well known equation [20, 21]

$$\lambda_0 = 2\mathcal{N}_0\tilde{J}^2 \int \frac{\langle P(\boldsymbol{q}, E)\rangle}{E}\,\mathrm{d}E. \tag{31}$$

One can estimate the factor λ on the Fermi surface as

$$\lambda \sim \frac{\mathcal{N}_0\tilde{J}^2}{T^*} = \frac{\varepsilon_F}{rT^*} \gg 1 \tag{32}$$

since the average spectral density of spin-fermion states is characterized by the bandwidth $\sim T^*$. Thus we conclude that the electron mass in certain conduction bands can be enhanced essentially by spinon scattering. This dynamical renormalization influences only the effective mass on the Fermi surface leaving intact the Fermi wave vector (see figure 3(*b*)). The fact that the dynamical mass enhancement does not violate the chemical potential provided $\partial\Sigma_R/\partial\varepsilon \gg v_F^{-1}\partial\Sigma_R/\partial p$ is well known in the Fermi liquid theory. However, the static scattering given by the diagrams of figure 1 open the possibility of Fermi surface reconstruction.

To show this we insert the enhanced density of states

$$\mathcal{N}(\epsilon) \approx \lambda\mathcal{N}_0(\epsilon) \tag{33}$$

in (18) for the scattering phase shift. One cannot expect large phase shift due to spinon scattering of bare electrons since the total number of unrenormalized states in the non-adiabatic layer of slow electrons is extremely small, $n_{slow} \sim T^*/\varepsilon_F$. However, due to the 'giant Migdal effect' [20] discussed above, a large enough number of electron states is sucked into this layer,

$$\tilde{n}_{slow} \sim \frac{1}{\ln^2(T^*/T_K)} \tag{34}$$

and the one-site static scattering can result in a noticeable phase shift. $\tilde{n}_{slow} < 1$ since $T^* > eT_K$ [15]. The excess density of states due to static spinon scattering is given by

$$\Delta\mathcal{N}(\epsilon) = \frac{1}{\pi}\frac{\mathrm{d}\delta(\epsilon)}{\mathrm{d}\epsilon} = \frac{\tilde{J}^2\mathcal{N}(\epsilon)}{[2 - \tilde{J}R(\epsilon)]^2 + [\pi\tilde{J}^2\mathcal{N}(\epsilon)]^2}\frac{\mathrm{d}R(\epsilon)}{\mathrm{d}\epsilon} \tag{35}$$

(spin degeneracy is not taken into account in this equation). Here $R(\epsilon)$ is the monotonically growing function provided there are no van Hove singularities close to the Fermi surface†, so $\Delta\mathcal{N}(\epsilon) > 0$ in the slow-electron layer, and the character of the dispersion law renormalization is asymmetric relative to the Fermi level unlike the case of the Migdal

† See, e.g., [27] where the properties of the Hilbert transform of the electron density of states are discussed in detail.

mechanism discussed above. Since the total number of electrons involved in this process $\tilde{n}_{slow} < 1$, the real resonance of Clogston type [24], i.e., the zero of the function $[2-\tilde{J}R(\epsilon)]$, cannot appear at the Fermi level, but, nonetheless, the electron dispersion curve in this layer flattens noticeably *as if* the resonance existed somewhere above the Fermi level. All these effects disappear for the electrons with the energy $\xi_p > T^*$ above the Fermi level, so the unrenormalized dispersion law is restored outside the non-adiabaticity layer. The general shape of the dispersion curve modified both by Migdal renormalization and static scattering is shown in figure 3(*c*).

Since the quasi-resonance level is pinned to the Fermi level, as in the case of Abrikosov–Suhl resonance discussed above, the change of the density of states described by (35) results in the shift of p_F. The magnitude of this shift can be evaluated as

$$\frac{\Delta p_F}{p_{F0}} = \frac{1}{r}\frac{\tilde{v}_F - v_F}{v_F} \tag{36}$$

where v_F is the Fermi velocity enhanced by Migdal renormalization and $\tilde{v}_F$ is the eventual velocity which is the result of the combined effect of the two mechanisms. When deriving (36), we used the linear dispersion law $\epsilon = \xi_p$ for both renormalized bands and defined p_F as $p_F = rT^*/v_F$. Then, taking for example the value of $r = 2$, one finds that a 30% increase of the radius of the Fermi sphere can be achieved by a rather modest enhancement factor $\tilde{v}_F/v_F = 1.6$.

Thus we come to a conclusion that the spinon renormalization of the electron density of states results not only in mass enhancement which turns out to be 'giant' in comparison with, e.g., non-adiabatic enhancement due to electron–phonon interaction (conventional Migdal effect), but also in swelling of the electron sheets of the Fermi surface (or in shrinkage of the hole pockets). Migdal-type renormalization gives the dominant contribution to the mass enhancement, but the static scattering can result in additional moderate increase of the effective mass.

One more effect of the static scattering given by (13), (15), and (18) can be essential for a pair of Bloch waves which become nearly degenerate close to the Fermi surface. This equation can be rewritten in a two-wave case as

$$(\epsilon - \epsilon_{k+g})(\epsilon - \epsilon_{k+g'}) - \Gamma^2_{gg'} = 0 \tag{37}$$

(extended zone notation is used). Since the scattering amplitude (13) enters the secular equation (15) instead of simple lattice potential (14), the strong $l = 2$ contribution given by (18) can result in anomalously large band splitting and, hence in noticeable mass renormalization and p_F shift (figure 4). In the multiband picture which is usual for HF systems such a situation seems to be not too uncommon.

To end the issue we return to the question of additional charge which appears under the Fermi surface in renormalized band calculations [9] discussed above. As in the case of resonance scattering, the shift of p_F corresponds to the increase of the occupied number of states under the Fermi surface. According to (35), the additional charge can be estimated as

$$\Delta n_c = \frac{1}{\pi}[\delta(\epsilon_F) - \delta(\epsilon_F - T^*)] \approx \tilde{n}_{slow}. \tag{38}$$

In the resonance theory the following sum rule is believed to be fulfilled [10, 28]:

$$\frac{\Omega_F}{(2\pi)^3} = n_c + n_f. \tag{39}$$

Here Ω_F is the volume under the Fermi surface of interacting electrons which should correspond to the number of both conduction electron states n_c plus the number of states

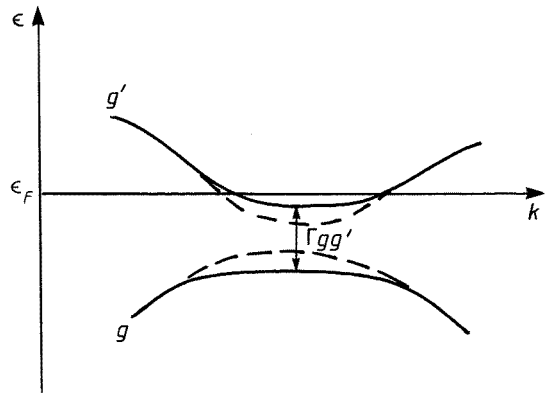

Figure 4. Two-wave mixing near the Fermi surface.

of the screened local moments n_f *provided* the screening is complete. The screening is, indeed, complete in the one-site Kondo model in accordance with (20) and (24): if one deals with a simple Kramers doublet, $\delta_\uparrow(\epsilon_F)+\delta_\downarrow(\epsilon_F)=\pi$. In the resonance approach the Kondo screening is assumed to take place in each unit cell of the Kondo lattice independently, so the Friedel–Nozières sum rule is transferred to the Kondo lattice model, and the Fermi surface swells as if an additional state arose under the Fermi level although this additional state is of purely spin origin. This effect is interpreted as a sort of dynamical recharging of resonating valence bonds due to Kondo coupling [14]. In the lattice case the resonance level ϵ_0 appears just above the Fermi level,

$$\epsilon_0 - \epsilon_F \sim V_0^2/D \approx T_K \tag{40}$$

and, as a result, $\Delta n_c + \Delta n_f$ is close to unity.

In our approach the Kondo scattering is quenched at high enough temperature $T^* > T_K$, thus the Kondo screening is incomplete, and the real Abrikosov–Suhl resonances are not formed. Instead, the 'underscreened' spin degrees of freedom are transformed into spin-fermion states which serve as a source of strong potential scattering for low-energy conduction electrons. Therefore, there is no charge promotion to the spin subsystem, and instead of the generalized sum rule (39) we return to the standard Luttinger theorem for conduction electrons, $n_c = 2\Omega_F/(2\pi)^3$. However, the potential scattering given by the diagrams of figures 1 and 2 can result in nearly the same effect as the resonance scattering *provided* the condition

$$2 - \tilde{J}R_\nu(\epsilon_F) \ll 1 \tag{41}$$

is fulfilled for a given band ν. The inequality (41) is not universal, and the part of spin scattering in formation of the Fermi surface depends both on the value of parameter $r = \ln(T^*/T_K)$ and on the magnitude of $R(\epsilon_F)$. The latter can be large enough only for the bands containing a strong contribution of the $d_{Ce,Ru}$ partial wave. The volume $\Omega_F^{(\nu)}$ of the corresponding sheet of the Fermi surface is expected to increase due to exchange interaction in accordance with figure 3 but only at the expense of the volumes of other sheets. Moreover, this electron overflow cannot change the compensation degree of the metal since no additional charge appears under the Fermi level when the exchange interaction is switched on. Thus, one can expect noticeable reconstruction of the Fermi surface only in the case

when the conduction electrons are distributed over several sheets of comparable capacity, and some of these sheets can serve as the source of electrons for others subject to strong remormalization. In the opposite case the giant Migdal effect will not be supported by noticeable reconstruction of the Fermi surface, and the dHvA measurements will detect enhanced electron masses given by (30) at the unreconstructed Fermi surface given by conduction electrons only.

The essential feature of the theory is the conclusion that the density of charged states $\mathcal{N}_c(\epsilon_F)$ should be less then the total density of fermion states $\mathcal{N}_{th}(\epsilon_F)$ seen as the Sommerfeld coefficient in the low-temperature specific heat γ_{th}. Using equations (30) and (32) one finds

$$\gamma_{th} = \gamma_{spinon} + \gamma_{el} = T^*(1 + r^{-1}). \tag{42}$$

Then the relation γ_{el}/γ_{th} can be estimated as

$$\frac{\gamma_{el}}{\gamma_{th}} = \frac{1}{1+r}. \tag{43}$$

Thus, in the case when only one electron band is strongly renormalized due to interaction with spin-fermion excitations, the contribution of heavy electrons to γ_{th} should not exceed 50%. This estimation does not take into account the contribution of lighter electrons, and the share of charged carriers grows noticeably provided several bands are subject to strong electron–spinon renormalization. If there are n renormalized electron masses of comparable magnitude, then the estimation (43) should be changed for

$$\frac{\gamma_{el}}{\gamma_{th}} = \frac{n}{n+r}. \tag{44}$$

The ratio γ_{el}/γ_{th} should also be influenced by an external magnetic field which perturbs both the electron and spinon spectrum.

It should be emphasized that unlike the approximation (4), (5) of the resonance theory the processes described by the diagrams of figures 1 and 2 do not violate the SU(2) gauge invariance of the Hamiltonian (1), and the results obtained do not depend on the approximations used in description of the RVB state. The only indispensable condition is the stabilization of RVB state against magnetic ordering of localized moments.

3. Renormalized electron bands and dHvA data for Ce-based heavy-fermion compounds

As was mentioned in the introduction, the de Hass–van Alphen effect is exclusively a useful tool for studying the electronic contributions to heavy-fermion thermodynamics, and there are several HF systems for which (i) the detailed experimental information on the structure of the Fermi surface is available, (ii) the experimental dHvA data on the shape of the Fermi surface are in reasonable correlation with the numerically calculated energy bands, and (iii) these data can be compared with those for the reference La-based systems. In this section these Ce-based compounds are considered from the viewpoint of applicability of the two-component HF liquid theory.

3.1. $CeRu_2Si_2$

The results of experimental dHvA studies of $CeRu_2Si_2$ [7, 8, 29, 30, 31] demonstrate coexistence of light and heavy carriers on the Fermi surface with effective masses varying from $1.0m_0$ to $140m_0$. According to these data, the multi-sheet Fermi surface consists of two

(or, maybe, three) concentric small light-hole pockets around the Z point of the Brillouin zone (bands 1–3), one large hole sheet with extremely heavy anisotropic mass $m^* > 100m_0$ centred at the same Z point (band 4), and one electron sheet of complicated structure formed mainly by the states near the Γ and X points of the Brillouin zone (band 5). Moderately heavy electron mass $\approx 20m_0$ was detected at this surface. The heavy masses are shown to be magnetic field dependent [30, 31], and these masses, apparently, disappear in a field $B > B_c$ where $B_c \approx 7.8$ T is a critical field applied parallel to the [100] direction where a steep metamagnetic crossover takes place.

Although the information about the dispersion laws and effective masses at the Fermi surface is not complete†, it is tempting to collect the contributions of various sheets to the total density of electronic states and compare the result with the data of thermodynamic measurements (Sommerfeld coefficient γ_{th}). Such an estimation was made in [31]. The assumed procedure used the results of the band calculations for the contribution of a given Fermi surface sheet $\mathcal{N}_i(\epsilon_F)$ as raw data and the enhancement coefficients $m^*_{i,exp}/m^*_{i,band}$ were taken from the dHvA experiment. It was found that the therodynamically measured Sommerfeld coefficient $\gamma_{th} = 350$ mJ mol^{-1} K^{-2} [32] correlates with the value collected from the dHvA data available, $\gamma_{el} = 260$ mJ mol^{-1} K^{-2}. Thus, according to these estimates

$$\gamma_{el} \approx 0.75\gamma_{th}. \tag{45}$$

It should be noted that the dominant contribution to this density of states comes from the large hole band 4 ($\gamma_{4,el} = 194 \pm 12$ mJ mol^{-1} K^{-2}), and the rest of the electron density of states is given by the electron band 5 which is highly anisotropic. Whereas there are at least three different cross sections of the band 4 which give large masses from $105m_0$ to $140m_0$ [31], the situation is much less clear with the band 5. There are three extremal orbitals with moderately enhanced masses from $20m_0$ to $12m_0$ which can be ascribed unambiguously to some cross sections of this surface, but up to now there is no confidence about uniform enhancement of the electron mass along the Fermi surface of this band (see [26, 31, 33] for discussion of the experimental situation). So the relation given by (45) should be considered as the estimation from above. Nevertheless, this result evidences that the charged degrees of freedom give the dominant contribution to the low-energy density of fermionic states in $CeRu_2Si_2$, so one should find out whether this result is compatible with the picture of renormalized electrons coexisting with neutral spin-fermions which was described in section 2.

It is useful to compare for this purpose the Fermi surfaces of $CeRu_2Si_2$ and its non-heavy-fermion analogue $LaRu_2Si_2$. The most striking difference between them is the change of the volume of the hole sheet 4. In the latter system this sheet centred in the Z point of the Brillouin zone is very large and contains 0.95 holes/cell [34]. This number should be compared with the value of 0.17 holes/cell in $CeRu_2Si_2$ [35]. Not only the shrinkage of this sheet but also the giant mass enhancement is observed in $CeRu_2Si_2$ (see above). These effects could be explained in principle by the mechanism described in the previous section (figure 3). According to the theory of electron–spinon scattering the band 4 (or 14 in the nomenclature of [33]) should be strongly renormalized because it is formed mainly by the d electrons of Ce and Ru sublattices for which the df exchange interaction responsible for the formation of spinon band is particularly strong, so one can expect both the giant Migdal effect which results in the mass enhancement given by (30), and the phase shift change (18) which is responsible for the Fermi sphere capacity change (24). However, the change of the Fermi surface volume is possible only at the expense of *other sheets* of the Fermi surface, so this effect can be realized provided there are at least two sheets of the

† The low value of B_c does not allow us to detect the cross sections of the heavy-mass sheets in a basal plane.

Fermi surface with comparable capacities. Unfortunately, this is, apparently, not the case in $CeRu_2Si_2$. Although the experimental information about the form and the volume of the second important part of the Fermi sphere, i.e. the electronic band 5, is still not complete, one can refer to the data for $LaRu_2Si_2$ in which this band contains only 0.06 electrons/cell, so there is no source of the carriers to fill the hole states in band 4 to the necessary degree.

Very important is the experimental information about the carrier compensation degree in $CeRu_2Si_2$. It should be reminded that $LaRu_2Si_2$ is an uncompensated material according to the magnetoresistance data [36]. If the heavy fermions in $CeRu_2Si_2$ are of purely spin origin then the f electrons remain localized, and this material should be still uncompensated. According to the magnetoresistance data for $CeRu_2Si_2$ presented in [36] the $\rho_\perp(H)$ behaviour reminds us of that for a compensated material, and this result was interpreted as an indication of the itinerant character of f electrons in this system. However, the recent magnetoresistance measurements demonstrate the change from H^2 to H dependence of $\rho_\perp(H)$ with growing field [37], so the question of the interpretation of transverse magnetoresistance seems to remain open. Nevertheless, the absence of large electron pockets in the Fermi surface of $LaRu_2Si_2$ indirectly points out that the spinon–fermion interaction cannot be the only source of conduction-band reconstruction in $CeRu_2Si_2$. Apparently, the f-electron charge fluctuations are not completely suppressed in this system, and dynamical sceening of local moments by these fluctuations can result in a dramatic change of the Fermi volume.

The situation with dHvA oscillations in the high-field phase above B_c [8, 30, 31] is challenging. Although the general shape and the volume of the large hole sheet ω which appears in this phase instead of the heavy-hole sheet (ξ, μ, ν) are compatible with predictions of the LDA band model in which the f electrons are treated in core states, the other branches which are expected to be observed for the f-core band structure are not seen in the high-field dHvA experiment. Moreover, the discrepancy between γ_{el} and γ_{th} becomes striking: the relation γ_{el}/γ_{th} is estimated as ~ 0.2 at 15 T. This means that either the general shape of the Fermi surface is changed drastically due to spin polarization, and some important heavy sheets are simply not seen yet, or the spin contribution to γ_{th} is dominant in the high-field phase. It should be noted, however, that the behaviour of a spin liquid in a high magnetic field demands careful theoretical investigation.

3.2. $CeCu_6$

$CeCu_6$ is the second HF compound where dHvA measurements are possible in the non-magnetic state. Unlike the case of $CeRu_2Si_2$, where the low-field and high-field phases are separated by sharp metamagnetic transition, in this material only a smooth crossover in the range 2.5 T$< B <$ 4.5 T takes place [38, 39]. In higher fields the intersite correlations seem to be suppressed as in $CeRu_2Si_2$ above B_c [39].

The detailed measurements of dHvA oscillations were made in the fields 4 T$< B <$ 14.5 T, i.e., in the 'high-field' state of this material [6, 40]. Unlike the case of $CeRu_2Si_2$, nearly all orbits seen in dHvA measurements have strongly enhanced electron masses in comparison with the non-correlated analogue $LaCu_6$. There are at least eight dHvA frequencies with the masses varying from $6m_0$ to $80m_0$. However, it turned out to be impossible either to put these frequencies in correspondence with dHvA branches in $LaCu_6$ or to attribute them to extremal orbits of LDA band calculations (both f band and f core).

One can refer to the extreme complexity of the Fermi surface in this low-symmetry material, and to various shortcomings which limit the applicability of the density functional calculation scheme to $CeCu_6$, but the strong renormalization of practically all conduction

bands in comparison with $LaCu_6$ seems to be a firmly established experimental fact. Such reconstruction does not contradict the predictions of two-component Fermi liquid theory.

The heavy masses demonstrate strong field dependence which reproduces nicely the field dependence of γ_{th} as in the high-field state of CeB_6 (see below). However, the attempt to estimate the density of states from dHvA experiments gave the value of $\gamma_{el} \approx 0.3\gamma_{th}$ in the range 10–13 T. One can conclude from this result that some heavier quasiparticles are not seen in the experiment, but the possibility of ascribing this discrepancy to the spin contribution to γ_{th} is also open.

To summarize, one can say that the data available do not rule out any mechanism of mass enhancement in $CeCu_6$, but these data also cannot be interpreted in favour of any theoretical approach.

3.3. CeB_6

Strictly speaking, cerium hexaboride is not the best object for application of the simple version of spin-liquid theory presented in this paper, first, because the ground state of the f shell is a quartet Γ_8 in this compound and the spin one-half description of the spinon band cannot be applied directly, and, second, because CeB_6 is antiferromagnetic in zero field and at low temperature $T < T_N = 2.3$ K. The dHvA data available were obtained for the high-field phase which shows quadrupolar ordering with a field induced antiferomagnetic component, so both the interpretation of these data in terms of the band-structure calculations using paramagnetic LaB_6 as a reference system and the applications of the paramagnetic spin-liquid model should be considered with caution. Nevertheless, there are many dHvA measurements for this compound which can be compared with the corresponding data for LaB_6. Important also is the fact that experimental data available give no indication of itinerant f-electron behaviour in this system.

In gross features the Fermi surface of CeB_6 as measured by the dHvA method correlates rather well with that of LaB_6 [6, 41, 42]. This result is more or less confirmed by the positron annihilation measurements in paramagnetic phase [43] although these data are obtained at $T = 30$ K which is too high to be able to judge about the heavy-fermion contribution to the Fermi surface. This surface consists of three nearly spherical ellipsoidal electron sheets formed by p-type boron bands and centred at the X points of the Brillouin zone and 12 small electron pockets on the diagonals of the Brillouin zone. The moderately heavy electron masses $m^* \approx 10$–$21m_0$ correspond to the cross sections of large electron ellipsoids. Thus, the main difference between the cases of $CeRu_2Si_2$ and CeB_6 is the conservation of both the volume and the shape of the p-electron Fermi surface in the latter case. This means that the mass enhancement is due rather to Migdal-type renormalization (30) than to Kondo-resonance hybridization (21). According to the above theoretical predictions, one cannot expect spinon scattering reconstruction of the heavy sheet of the Fermi surface because there is no second large electron sheet in this system which could be the source of the carriers necessary for such reconstruction.

Then, if mass enhancement in CeB_6 is due to interaction with virtual spin–fermion pairs described by the polarization operator (26) (not charged fermion pairs and not Bose-type spin fluctuations), one should expect the discrepancy between γ_{el} and γ_{th}. Indeed, the comparison of the quasiparticle density of states, as given by three large and 12 small electron ellipsoids, with the thermodynamic density of states results in a discrepancy between γ_{el} and γ_{th} which reaches 100% in the external field of 10 T and diminishes with growing field according to the estimations presented in [44]. To improve the situation these authors have taken into account the contribution of the neck regions which could not be measured by dHvA but

were estimated theoretically by using the known data for the sizes of large ellipsoids. This procedure gave the desired correlation although nearly the half of the value of γ_{el} is still beyond the experimental control. Very recently new extremal orbitals were found for CeB_6 in the anti-quadrupolar phase [45], so the fitting procedure should be visited once more.

Thus the situation in CeB_6 is still unclear although the well established experimental data for the high-field are compatible with giant Migdal renormalization of electron mass. One can say, however, that the main difference between $CeRu_2Si_2$ and CeB_6 is the conservation of all features of the p-electron Fermi surface of the latter in the high-field phase.

3.4. $CeAl_2$ and $CeIn_3$

These two materials have much in common. Both of them can be classified as Kondo lattice systems with moderately heavy-fermion behaviour ($\gamma_{th} = 135$ mJ K^{-2} mol^{-1} in $CeAl_2$ and 130 mJ K^{-2} mol^{-1} in $CeIn_3$). For both of them the localized behaviour of Ce magnetic moments is well established.

$CeAl_2$ orders antiferromagnetically at $T_N = 3.8$ K, and the dHvA measurements are made at $B > B_c = 5.27$ T in a high-field phase above the metamagnetic transition [29, 46]. These measurements demonstrated striking similarity between the Fermi surfaces in $CeAl_2$ and sister compound $LaAl_2$, although the moderately heavy masses of $\approx 15m_0$ were registered at least for two electron sheets. The mass enhancement seen from dHvA measurements is systematically lower than the γ_{th} enhancement over the corresponding value of $LaAl_2$ ($\sim 20\%$ deficit).

$CeIn_3$ orders antiferromagnetically at $T_N = 10.2$ K and does not undergo the metamagnetic transition at $B < 15$ T [47]. As the f electrons in $CeIn_3$ are known to be well localized, the topology of the Fermi surface is expected to be similar to that of $LaIn_3$, although some parts of it could be folded into smaller bands in the magnetically ordered state. This picture is confirmed in general by dHvA experiments [48], but the absence of the band calculations for antiferromagnetic state makes direct comparison difficult. Moderately heavy masses ($11.2m_0$ and $20.7m_0$) are registered, but the share of these masses in γ_{th} is not estimated. Careful investigation of Fermi surface of this system in magnetic state is highly desirable, since this is the only material among magnetic Kondo lattices where the dHvA measurements are possible below the metamagnetic transition.

4. Conclusions

Although the de Haas–van Alphen oscillations give direct information about the electron mass enhancement, the task of separating the pure contribution of spin excitations from the electron enhancement effects in the low-temperature thermodynamics and magnetic response of the heavy fermion systems is extremely difficult. The problems arise both in the theoretical analysis and in the choice of experimental objects.

Three theoretical possibilities for explaining the origin of heavy fermions exist: (i) enhancement of electron–polaron, paramagnon, etc type for *itinerant* f electrons with heavy enough 'bare' masses; (ii) many-particle Kondo-resonance renormalization of electron dispersion law which results in a change of the Fermi volume because of charging of the spin excitations due to Kondo coupling; (iii) spinon–electron interaction in the state where the (neutral) f-spin-fermion degrees of freedom are separated from (charged) conduction electron degrees of freedom. The first possibility can be realized only for a system with essentially non-integer valence of the f shell, thus ruling out the possibility of explaining the heavy-fermion behaviour in systems with integer valence of Ce ions. Two other possibilities give

a real alternative for explaining the HF behaviour of many Ce-based systems. To choose between these approaches the careful analysis of compensation degree and the thorough determination of the difference between the diamagnetic and thermodynamic densities of states is necessary.

Unfortunately, one cannot point out a system where the dHvA measurements allow one to choose between two latter models. The most thoroughly studied compound $CeRu_2Si_2$ seems to behave rather more like the system with itinerant f electrons than that with the localized f moments at least in moderate external magnetic fields. One should emphasize, however, that the properties of this system above the metamagnetic transition cannot be described either by the itinerant band model or by the Kondo-resonance model. Another interesting object, the $CeCu_6$ compound, has too complicated a band structure to make definite experimental conclusions. All other heavy-fermion systems where large effective masses were detected experimentally in dHvA measurements (CeB_6, $CeAl_2$, $CeIn_3$) have magnetic ground states, and the experimental information available was obtained for the high-field phases. These latter Kondo-lattice systems demonstrate noticeable mass enhancement without Fermi surface reconstruction in comparison with La-based prototypes. One can interpret this fact as an indication of absence of resonance scattering effect in the high-field state and ascribe the mass enhancement to Migdal-type self-energy corrections, although the nature of the slow quasiparticles responsible for mass enhancement is still a matter for discussion.

Acknowledgments

This work was completed during the author's stay in the Cavendish Laboratory of Cambridge University. The visit was funded by the Royal Society in the framework of the Kapitza Award. The author is greatly indebted to Professor G Lonzarich and Dr D Khmelnitskii for their hospitality and permanent support. Discussions with M A Alam, S Julian, G McMullen, M Springford, and F S Tautz were highly useful for clarifying the experimental situation. The work was partially supported by the International Scientific Foundation (grant MBH300), the International Association INTAS (grant 93-2834) and the Dutch Scientific Research Organization NWO (grant 07-30-002).

References

[1] Onuki Y and Hasegawa A 1992 *J. Magn. Magn. Mater.* **108** 19
[2] Kagan Yu, Kikoin K A and Prokof'ev N V 1992 *Physica* B **182** 201
[3] Taillefer L and Lonzarich G G 1988 *Phys. Rev. Lett.* **60** 1570
[4] Schmiedeshoff G M, Fisk Z and Smith J L 1994 *Phys. Rev.* **49** 658
[5] Hunt M, Meeson P, Probst P-A, Reinders P H P, Springford M, Assmus W and Sun W 1990 *J. Phys.: Condens. Matter* **2** 6859
[6] Chapman S, Hunt M, Meeson P, Reinders P H P, Springford M and Norman M 1990 *J. Phys.: Condens. Matter* **2** 8123
[7] Aoki H, Uji S, Albessard A K and Onuki Y 1993 *Phys. Rev. Lett.* **71** 2110
[8] Julian S R, Tautz F S, McMullan G J and Lonzarich G G 1994 *Physica* B **199–200** 63
[9] Zwicknagl G 1992 *Adv. Phys.* **41** 203
[10] Martin R M 1982 *Phys. Rev. Lett.* **48** 362
[11] Coleman P 1983 *Phys. Rev.* B **28** 5255
[12] Razafimandimby H, Fulde P and Keller J 1984 *Z. Phys.* B **54** 111
[13] Hewson A C 1993 *The Kondo Problem to Heavy Fermions* (Cambridge: Cambridge University Press)
[14] Coleman P and Andrei N 1989 *J. Phys.: Condens. Matter* **1** 4057
[15] Kikoin K A, Kiselev M N and Mishchenko A S 1994 *JETP Lett.* **60** 600

[16] Doniach S 1977 *Physica* B **91** 231
[17] Lee P A and Nagaosa N 1992 *Phys. Rev.* B **46** 5621
[18] Fulde P and Jensen J 1983 *Phys. Rev.* B **27** 4085
[19] Varma C 1985 *Phys. Rev. Lett.* **55** 2723
[20] Eliashberg G M 1987 *JETP Lett.* **45** 35
[21] Kagan Yu, Kikoin K A and Prokof'ev N V 1992 *JETP Lett.* **57** 219
[22] Kagan Yu and Prokof'ev N V 1993 *J. Phys.: Condens. Matter* **5** 6189
[23] Khaliullin G G 1994 *Sov. Phys.–JETP* **79** 473
[24] Clogston A M 1962 *Phys. Rev.* **125** 439
[25] Ziman J M 1971 *Solid State Physics* vol 26, ed H Ehrenreich, F Seitz and D Turnbull (New York: Academic) p 1
[26] Runge E K R, Albers R C, Christensen N E and Zwicknagl G E 1995 *Phys. Rev.* B **51** 10 375
[27] Economou E N 1983 *Green's Functions in Quantum Physics* (Berlin: Springer)
[28] Coleman P 1995 *Physica* B **206–207** 872
[29] Lonzarich G G 1988 *J. Magn. Magn. Mater.* **76–77** 1
[30] Aoki H, Uji S, Albessard A K and Onuki Y 1993 *J. Phys. Soc. Japan* **62** 3157
[31] Tautz F S, Julian S R, McMullan G J and Lonzarich G G 1995 *Physica* B **206–207** 29
[32] van der Meulen H P, de Visser A, Franse J J M, Berendschot T T J M, Perenboom J A A J, van Kempen H, Lacerda A, Lejay P and Flouquet J 1991 *Phys. Rev.* B **44** 814
[33] Yamagami H and Hasegawa A 1993 *J. Phys. Soc. Japan* **62** 592
[34] Yamagami H and Hasegawa A 1992 *J. Phys. Soc. Japan* **61** 2388
[35] Tautz F S 1994 *PhD Thesis* Cambridge University
[36] Onuki Y, Umehara I, Albessard A K, Ebihara T and Satoh K 1992 *J. Phys. Soc. Japan* **61** 961
[37] Kambe S, Suderow H, Flouquet J, Haen P and Lejay P 1995 *Solid State Commun.* **95** 449
[38] Amato A, Jaccard D, Flouquet J, Lapierre F, Tholence J L, Fisher R A, Lacy S E, Olsen J A and Phillips N E 1987 *J. Low Temp. Phys.* **68** 371
[39] Rossat-Mignot J, Regnault L, Jacoud J, Vettier C, Lejay P, Flouquet J, Walker E, Jaccard D and Amato A 1988 *J. Magn. Magn. Mater.* **76–77** 295
[40] Springford M 1991 *Physica* B **171** 151
[41] Joss W, van Ruitenbeek J M, Grabtree G W, Tholence J L, van Deursen A J P and Fisk Z 1986 *Phys. Rev. Lett.* **57** 1631
[42] Onuki Y, Komatsubara T, Reinders P H P and Springford M 1989 *J. Phys. Soc. Japan* **58** 3698
[43] Biasini M, Alam M A, Harima H, Onuki Y, Fretwell H M and West R N 1994 *J. Phys.: Condens. Matter* **6** 7823
[44] Harrison N, Meeson P, Probst P-A and Springford M 1993 *J. Phys.: Condens. Matter* **5** 7435
[45] Springford M 1995 private communication
[46] Reinders P H P and Springford M 1989 *J. Magn. Magn. Mater.* **79** 295
[47] Onuki Y and Hasegawa A 1992 *J. Magn. Magn. Mater.* **108** 19
[48] Satoh K, Umehara I, Nagai N, Onuki Y, Sakamoto I, Hunt M, Meeson P, Probst P-A and Springford M 1992 *J. Magn. Magn. Mater.* **104–107** 1411